Intravoxel Incoherent Motion for Differentiating Spinal Metastasis: A Pilot Study

Yuan Li
Peking University Third Hospital
Xiaoying Xing
Peking University Third Hospital
Enlong Zhang
Peking University International Hospital
Siyuan Qin
Peking University Third Hospital
Huishu Yuan
Peking University Third Hospital
Ning Lang (langning800129@126.com)
Peking University Third Hospital

Research Article

Keywords: Intravoxel incoherent motion, Diffusion, Magnetic resonance imaging, Metastasis, Spine

Posted Date: May 19th, 2021

DOI: https://doi.org/10.21203/rs.3.rs-495875/v1

Abstract

Background: To investigate the value of an intravoxel incoherent motion (IVIM) MRI for discriminating spinal metastasis from tuberculous spondylitis.

Methods: This study included 50 patients with spinal metastasis (32 lung cancer, 7 breast cancer, 11 renal cancer), and 20 tuberculous spondylitis. All patients underwent IVIM MRI at 3.0T before treatment. The IVIM parameters including single-index model (Apparent diffusion coefficient (ADC)-stand), double exponential model (ADC_{slow}、ADC_{fast} and f) and stretched-exponential model parameters (distributed diffusion coefficient (DDC) and α) were acquired. Two radiologists separately measured these parameters for each lesion through drawing region of interest. Receiver operating characteristic (ROC) and the area under the ROC curve analysis was used to evaluate the diagnostic performance. Each parameter was substituted into the Logistic regression model to determine the meaningful parameters, and the combined diagnostic performance was evaluated.

Results: The ADC_{fast} and f showed significant differences between spinal metastasis and tuberculous spondylitis. (for all, $p < 0.05$). The Logistic regression model results showed that ADC_{fast} and f were independent factors affecting the conclusion ($P<0.05$). The AUC values of ADC_{fast} and f were 0.823 (95%CI:0.719 to 0.927) and 0.876 (95%CI: 0.782 to 0.969), respectively. ADC_{fast} combined with f showed the highest AUC value of 0.925 (95%CI: 0.858 to 0.992). Additional significant differences were found in ADC_{stand}, $ADC_{slow,}$ DDC and α among different metastasis type.

Conclusions: IVIM MR imaging may be helpful for differentiating spinal metastasis from tuberculous spondylitis and may be used to detect the origin tumor for those patients who could not identify primary tumors, and provide help for clinical treatment.

Background

Osteoporosis, trauma, infection, or tumors are typically causes of clinically common diseases of the spine. Its diagnosis mainly depends on imaging findings and clinical features. But benign and malignant lesions in the spine may have similar imaging findings, especially in the early stages of the disease[1]. In addition, with the increasing incidence of cancer in modern society, the diagnosis of spinal bone lesions becomes more and more difficult. Spine is a site of metastasis in 10–15% of cancers, which is the third most common site for cancer cells to metastasize[2] and spinal metastases are the most common tumors of the spine[3]. The most common cancer that causes metastases to the spine is lung cancer, breast cancer and renal cancer. The major differential diagnoses for spinal metastases include spinal tuberculosis. Spinal metastases and tuberculosis with typical and specific imaging findings are relatively easy to diagnose correctly. However, most of the clinical presentation between them are usually not characteristic, leading to misdiagnosis. Besides, the image features of different diseases have some overlap. Therefore, an effective differential diagnosis method to identify different lesions in the spine is of great significance in clinical practice[4]. In addition, for patients with spinal metastases, it is important

to treat the primary lesion as well as the metastatic tumor. The treatment of metastatic tumors from different sources is also different, so it is possible to infer the type of primary lesion based on the imaging findings of spinal metastatic tumors, which may provide assistance for clinical treatment. Because the clinical course, prognosis and treatment strategy of different types of spinal metastatic and spinal tuberculosis differ greatly, the differential diagnosis of them is difficult and should be accurate diagnosis to improve patients' quality of live.

Intravoxel incoherent motion (IVIM) is a noninvasive MRI method to visualize microscopic motions of water, refers to translational motion that presents a velocity direction and/or amplitude distribution within a given voxel and over a measured time[5]. Water molecular diffusion and perfusion-related diffusion can be achieved by allowing monitoring the extraction of molecular diffusion coefficients (ADC_{slow}), the perfusion-related diffusion (ADC_{fast}), and perfusion fraction (f). Recently, it has been used to estimate tissue water diffusivity and micro-capillary perfusion. Perfusion MRI based on IVIM, which does not require contrast agents, has been widely used in studies of oncology. IVIM has been reported for glioma grading, tumor diagnosis, central nervous system and abdomen since its development over the past years[6–10].

It was reported that IVIM may help to differentiate malignant spinal tumors from acute vertebral compression fractures and tuberculous spondylitis[4] and IVIM-DWI could make for the early diagnosis of ductal carcinoma in situ of the breast, and reduce the misdiagnosis and over-treatment of benign lesions[11]. IVIM and conventional radiologic features improve preoperative assessment of microvascular invasion in patients with hepatocellular carcinoma[12]. IVIM-DWI-derived parameters, especially the pseudo diffusion coefficient, were related to tumor grade and stage in rectal cancer patients, and the difference between subjects with extramural vascular invasion and those without extramural vascular invasion was statistically significant. IVIM-DWI derived parameters would help to predict tumor aggressiveness and prognosis[13]. IVIM MRI quantitatively measures local microvascular muscle perfusion to detect muscle activation patterns through walking and running[14]. Zhu G et al. reported that IVIM with these b values (0, 50, 200, 1000) collects diffusion and perfusion information from a single short MRI sequence, which may have important implications for the imaging of acute ischemic stroke patients[15].

Accordingly, our aim was to investigate the IVIM parameters in spinal diseases and to discriminate spinal metastasis from tuberculous spondylitis and to investigate the feasibility of tumor type differential diagnosis of different metastases, including lung cancer, breast cancer and renal cancer.

Methods

Patients

This retrospective study was approved by the standards of the local ethics committee, with waiver of informed consent granted. This study included 50 patients with spinal metastasis (32 lung cancer, 7 breast cancer, 11 renal cancer), and 20 tuberculous spondylitis from Peking Third Hospital (Beijing, China) with histopathological diagnosis. All patients underwent IVIM MRI at 3.0T before treatment and puncture.

MRI acquisitions

Scanning was performed using a 3.0T MRI system (GE Healthcare 750) and 8-channel spinal coils. Conventional MRI sequence scanning was performed to help lesion localization. For patients with multiple lesions, lesions with the largest diameter were selected for DWI scanning. Conventional MRI sequences included axial and sagittal fast recovery fast spin echo (FRFSE) sequence T2 WI) with a repetition time (TR) 2800 ~ 4341 ms, echo time (TE) 98 ~ 142ms, slice thickness of 3.0mm, slice gap of 0.3mm, band width of 62.5 kHz, field of view (FOV) of 20 cm × 20 cm ~ 36 cm × 36 cm, matrix of 288 × 288 (axial) and 488 × 320 (sagittal). Sagittal FSE sequence T1WI FSE with a TR of 500 ~ 642ms, TE of 8 ~ 11 ms, slice thickness of 3. 0 mm, slice gap of 0. 3 mm, bandwidth of 62.5 kHz, FOV of 28 cm × 28 cm ~ 36 cm × 36 cm, matrix of 320 × 320. Cervical and thoracic sagittal position IDEAL sequence T2 WI: TR of 3000 ms, TE of 69 ms, slice thickness of 30 m, slice gap of 0.3 mm, band width of 833 kHz, FOV of 28 cm × 28 cm ~ 36 cm × 36 cm; matrix of 320 × 192; Lumbar and Sacro coccyx lipid suppression FRFSE sequence T2 WI: TR of 2409 ~ 3100 ms TE of 88 ~ 98 ms, slice thickness of 3. 0 mm, slice gap of 0. 3 mm, bandwidth of 50.0 kHz, FOV of 28 cm × 28 cm ~ 36 cm.

IVIM-DWI was obtained with an axis single excitation spin echo plane echo imaging sequence, and the parameters were as follows: TR of 3000 ms TE of 64 ms, slice thickness 4.0 mm, layer spacing 0.4 mm, bandwidth of 250. 0 kHz, FOV of 24 cm × 24 cm, matrix 128 × 64. b values of 0, 20, 50, 100, 150, 200, 400, 800, 1200, 1500 s/mm^2, and the excitation times were 2, 2, 2, 1, 1, 1, 2, 4, 6, 8. The scanning time was 252 s.

Regions of interest

The region of interest (ROI) was set in the center of the lesion with an area of 30–100 mm^2[16] and the solid components of the tumor were included as much as possible avoiding the lesion edge, necrosis, bone cortex, and blood vessels. The analysis was performed independently by two radiologists (initials: EZ, XX) with more than 5 years of experience on the GE AW4.5 workstation, and the average of the ROI measurements for each parameter was taken as the final measurement result.

Post-processing and MR Imaging analysis

All data were transferred to an imaging workstation for analysis. The IVIM parameters including single-index model (Apparent diffusion coefficient (ADC)-stand), double exponential model (ADC_{slow},ADC_{fast} and perfusion fraction (f)) and stretched-exponential model parameters (distributed diffusion coefficient (DDC) and intravoxel water diffusion heterogeneity (α)) were acquired. Two radiologists separately measured these parameters for each lesion through drawing region of interest. Receiver operating

characteristic (ROC) and the area under the ROC curve (AUC) analysis was used to evaluate the diagnostic performance.

The ADC value was obtained by using high and low b values monoexponentially fitted to the following equation: Sb = S0 × exp (-b × ADC), where Sb is the signal intensity observed in the absence of a diffusion gradient. The formula for the biexponential model was calculated as follows: Sb = S0 × [(1- f) × exp (-b × ADC_{slow}) + exp (b× ADC_{fast})], where S0 is the mean signal intensity, ADC_{slow} is the molecular diffusion coefficient, ADC_{fast} is the perfusion-related coefficient, and f is the perfusion fraction. The formula for the stretched-exponential model is as follows: Sb = S0 × exp (-b × DDCα), where DDC is a distributed diffusion coefficient, and α reflects the diffusion heterogeneity of water molecules in voxels.

Statistical analysis

All statistical analyses were performed using SPSS version 22.0 (SPSS, Inc., Chicago, IL, USA). Continuous variables are expressed as the mean ± standard deviation. The intraclass correlation coefficient (ICC) was used to analyze the agreement between the two radiologists and was interpreted as follows: 0.00-0.20, poor agreement, 0.21–0.4, fair agreement, 0.41–0.60, moderate agreement, 0.61–0.80, good agreement, and 0.81-1.00, excellent agreement. Categorical variables are expressed as percentage with 95% confidence interval (CI). Two independent samples t-tests were used to compare normal distribution data, and the Mann-Whitney U test were used to compare nonmoral distribution data. Date in different spinal metastasis groups were compared using the one-way ANOVA. The variables with statistical significance in univariate analysis were included in the multivariate Logistic regression model. Nonparametric ROC analysis was performed to evaluate the diagnostic performance of the IVIM parameters. The AUC was calculated to investigate the performance of these parameters, and the cut-off values with the largest sum of sensitivity and specificity were calculated from the ROC curves. The significance level set at $p < 0.05$.

Results

Patients

There were 50 patients with spinal metastasis (32 lung cancer, 7 breast cancer, 11 renal cancer), means age ± standard deviations: 56.92 ± 9.29 years, and 20 tuberculous spondylitis (means age ± standard deviations: 48.82 ± 19.84 years). The participants' basic information was provided in table 1. Figs. 1–2 shows IVIM imaging and the measurement methods for representative cases of spinal metastasis from lung cancer and tuberculosis.

Interobserver reproducibility for MRI measurement

Excellent interobservers (initials: EZ and XX) reproducibility was obtained for ADC_{stand}, ADC_{slow}、ADC_{fast}, f values, DDC and α, with ICC value was 0.929 (95%CI: 0.889 to 0.956), 0.946 (95%CI: 0.914–0.966), 0.849

(95%CI: 0.768 to 0.903), 0.868 (95%CI: 0.796 to 0.916), 0.924 (95%CI: 0.880 to 0.952), and 0.911 (95%CI: 0.860 to 0.944), respectively.

Comparison of IVIM parameters among different groups

Mean values of ADC_{stand}, ADC_{slow}、ADC_{fast}, f, DDC and α of tuberculous spondylitis and spinal metastasis are described in Table 2. The results showed the ADC_{fast} of spinal metastasis was significantly higher compered to tuberculous spondylitis, and lower f values in patients with spinal metastasis compered to tuberculous spondylitis (for all, $p < 0.05$) (Table 3). The mean ADC_{stand}, ADC_{slow}, DDC and α values between spinal metastasis and tuberculous spondylitis did not reach statistical significance. Additional significant differences were found in the ADC_{stand}, $ADC_{slow,}$ DDC and α among different metastasis type (for all, $p < 0.05$) .

Logistic regression model

The variables with statistical significance in univariate analysis and those that were considered to have influence on the outcome were included in the multivariate Logistic regression model, and the results showed that ADC_{fast} and f were independent variables affecting the conclusion ($p < 0.05$) (Table 4).

ROC-analysis

In the ROC-analysis for differentiation of spinal metastasis and tuberculous spondylitis, AUC values of ADC_{fast} and f were 0.876 (95% CI, 0.782 to 0.9969) and 0.823 (95% CI, 0.719 to 0.927), respectively. The sensitivity and specificity of ADC_{fast} value to differentiate spinal metastasis and tuberculous spondylitis were 80.0% and 85.0%. The sensitivity and specificity of f value were 86.0% and 65.0%. ADC_{fast} combined with f showed much higher AUC than ADC_{fast} and f, which the AUC values were 0.925 (95% CI, 0.858 to 0.992). By using the ADC_{fast} combined with f as a discriminative index for the discrimination of spinal metastasis from tuberculous spondylitis, the sensitivity and specificity were 94.0% and 80.0% (Table 5, Fig3).

Discussion And Conclusions

IVIM method is a diffusion-weighted MRI sequence used to estimate perfusion parameters, which has several advantages over commonly used methods. It is a non-invasive alternative to perfusion measurement, eliminating the need for intravenous injection of exogenous contrast agent through a single image sequence, reducing examination time. In addition, its signal is highly spatially specific because it comes primarily from a place where measurements are taken independently of the arterial blood flow path before reaching there. Finally, it provides additional information compared to ASL, and the combination of the two approaches can be used for the assessment of neurological diseases[17].

It recently reported that the IVIM parameters could help to more precisely assess the early diagnosis and differentiation of diseases, as well as quantitatively monitor the effectiveness of treatment for tumors

and other diseases. Ding Y etl.[18] compare the diagnostic values of IVIM, conventional DWI, and diffusion kurtosis imaging (DKI) in differentiating between benign and malignant renal tumors. They found the D value is the best parameter for differentiating cell renal cell carcinoma (ccRCC) from benign renal tumors. The f value is the best parameter for differentiating non-ccRCC from benign renal tumors. IVIM parameters are the best, while DWI and DKI parameters have similar performance in differentiating malignant and benign renal tumors. Another article found that rectal cancers with different KRAS mutation statuses had distinctive diffusion/perfusion characteristics. D values were lower in the KRAS mutant group. A higher D* value was demonstrated in the KRAS mutant group. IVIM MRI may potentially help preoperative KRAS mutant status prediction[19]. Zhu L etl. [20] evaluated the performance of tumor size and IVIM-derived parameters in predicting long-term prognosis, found that IVIM MR imaging has great potential in predicting long-term prognosis in patients with advanced cervical cancers treated with concurrent chemo-radiotherapy.

In early or atypical spinal tuberculosis, there is no typical obvious bone erosion or abscess, and the imaging findings are complex and sometimes similar to tumors, leading to misdiagnosis. While this is not common, it is still necessary to find ways to avoid it. Within the spinal column, metastasis is more commonly found in the thoracic region, followed by the lumbar region, while the cervical region is the least likely place professionals find metastasis. The aim of this study is to evaluate the performance diagnostic values of IVIM MRI for differentiating spinal metastasis. To the best of our knowledge, our investigation is the first to illustrate the IVIM relative parameters for differentiation of spinal tuberculosis and spinal metastasis.

Our results shown that some IVIM parameters could help discriminate spinal metastasis from tuberculous spondylitis and could investigate the feasibility of tumor type differential diagnosis of different metastases, including lung cancer, breast cancer and renal cancer. Conventional DWI is based on the micro-movement of water molecules, which reflects the speed of water diffusion in the tissue. ADC values can quantitatively evaluate tissue diffusion and show microscopic changes at the cellular level caused by pathophysiological changes. In our study, no significant difference in ADC values was found between spinal metastases and tuberculous spondylitis, suggesting an ADC overlap in distinguishing them. Therefore, the results show that the role of traditional ADC DWI in differentiating benign and malignant lesions of the spine is limited, which is consistent with previous studies[4, 21–22] .

It is known that the ADC_{slow} is mainly affected by water molecule diffusion of the lesion tissue and ADC_{fast} is mainly affected by capillary microcirculation perfusion. Our results showed the ADC_{fast} value of spinal metastases was significantly higher than that of tuberculous spondylitis, which suggests that perfusion greatly increases. However, no significant differences were found between the ADC_{slow} values between them. But the ADC_{slow} value of spinal metastasis with lung cancer was significantly lower than that of spinal metastasis with breast cancer as well as with renal cancer, suggesting that true diffusion is more restricted in lung cancer than breast cancer and renal cancer. ADC_{fast} and f values except for ADC_{slow} value showed better diagnostic performance than ADC value for differentiating spinal

metastasis and tuberculous spondylitis. The f value is mainly affected by the blood volume of microcirculation perfusion, reflecting the proportion of microcirculation perfusion in tissue diffusion. Our results showed that f value of spinal metastasis was lower than that of tuberculous spondylitis group. Similar findings have been found in nasopharyngeal, pancreatic, and cervical lymph node metastases in previous studies[23–24]. The reasons might be the high cell density of spinal metastasis, the microvessels in the intercellular stroma were compressed, and the new vessels in malignant lesions were compressed, deformed and branched disorderly, leading to the decrease of the proportion of microperfusion components. In our study, ADC_{fast} combined with f showed much higher AUC than ADC_{fast} and f. these finding suggested that ADC_{fast} combined with f was more valuable for the differential diagnosis of spinal metastasis and tuberculous spondylitis.

The DDC and α value reflects the heterogeneity of diffusion in the tissue. The value of α is set between 0 and 1. The closer the α value is to 1, the higher the homogeneity of the diffusion component is; the closer the α value is to 0, the higher the heterogeneity of the diffusion component is and the more complex the diffusion component is. In this study, the DDC and α value of spinal metastasis was lower than that of tuberculous spondylitis. however, there was no significant. indicating that compared with tuberculous spondylitis, malignant tissue is more complex and heterogeneous, which leads to the decrease of DDC and α value. Additional significant differences were found in the ADC_{stand}, ADC_{slow}, DDC and α among different metastasis type. The reasons for the above results may be related to the pathophysiological changes of the disease and the theory behind different imaging techniques.

Although with novel findings, our study also has some limitations, which we would further improve in the future work. Firstly, the small sample size of spinal metastasis and tuberculous spondylitis. Secondly, All values were measured by manual outlining ROI, and the ROI was placed on the solid components of the tumor to calculate the average value. Although it was representative to some extent, it was not conducive to the evaluation of tumor heterogeneity. Thirdly, IVIM technology itself is not stable. So far there is no specific standard about multiple b value of IVIM sequences, and the calculations still need further exploration[25].

In conclusion, IVIM MR imaging may be helpful for differentiating spinal metastasis from tuberculous spondylitis and provide help for clinical treatment. The combined ADC_{fast} and f parameters are better than ADC_{fast}, and f. Despite the small patient population, this study may lead to further developments in the application of IVIM in differentiating benign and malignant spinal skeletal lesions.

Abbreviations

IVIM: Intravoxel incoherent motion; ADC:Apparent diffusion coefficient; DDC:Distributed diffusion coefficient; ROC:Receiver operating characteristic; AUC:Areas under the curves; ICC:Intraclass correlation coefficient; CI:Confidence interval; f:Perfusion fraction; TR:Repetition time; TE:Echo time; FOV:Field of view; ROI:Region of interest; DWI:Diffusion-weighted imaging; DKI:Diffusion kurtosis imaging; ccRCC:Cell renal cell carcinoma

Declarations

Ethics approval and consent to participate

Institutional Review Board approval of Peking University Third Hospital was obtained. Informed consent was exempted by the Institutional Review Board of Peking University Third Hospital because of the retrospective nature of this study. All methods were performed in accordance with the 1964 Helsinki declaration and its later amendments or comparable ethical standards.

Consent for publication

Not applicable.

Availability of data and materials

The datasets used and/or analyzed during the current study are available from the corresponding author on reasonable request.

Competing interests

The authors declare no conflicts of interest for this work.

Funding

This study has received funding by National Natural Science Foundation of China (No. 81971578; 81901791; 81871326); Beijing Natural Science Foundation (No. Z190020); Peking University International Hospital Research Grant (No. YN2019QN03).

Authors' Contributions

YL and XYX conceived and designed the experiments; YL and ELZ performed the experiments; YL and ELZ analyzed the data and wrote the manuscript; SYQ contributed materials and analysis tools and performed statistical analysis; NL and HUY contributed to discussions, interpretation of the data and revision of the manuscript. All authors reviewed and approved the final manuscript.

Acknowledgements

Not applicable.

References

1. Thawait SK, Marcus MA, Morrison WB, Klufas RA, Eng J, Carrino JA. Research synthesis: what is the diagnostic performance of magnetic resonance imaging to discriminate benign from malignant vertebral compression fractures? Systematic review and meta-analysis[J]. Spine (Phila Pa 1976) 2012, **37**(12)**:** E736-E744.

2. Witham TF, Khavkin YA, Gallia GL, Wolinsky JP, Gokaslan ZL. Surgery insight: current management of epidural spinal cord compression from metastatic spine disease[J]. Nat Clin Pract Neurol 2006, **2**(2)**:** 87-94, 116.
3. Mundy GR. Metastasis to bone: causes, consequences and therapeutic opportunities[J]. NAT REV CANCER 2002, **2**(8)**:** 584-593.
4. Chen Y, Yu Q, La Tegola L, Mei Y, Chen J, Huang W, Zhang X, Guglielmi G. Intravoxel incoherent motion MR imaging for differentiating malignant lesions in spine: A pilot study[J]. EUR J RADIOL 2019, **120:** 108672.
5. Le Bihan D. What can we see with IVIM MRI[J]? NEUROIMAGE 2019, **187:** 56-67.
6. Federau C, O'Brien K, Meuli R, Hagmann P, Maeder P. Measuring brain perfusion with intravoxel incoherent motion (IVIM): initial clinical experience[J]. J MAGN RESON IMAGING 2014, **39**(3)**:** 624-632.
7. Shen N, Zhao L, Jiang J, Jiang R, Su C, Zhang S, Tang X, Zhu W. Intravoxel incoherent motion diffusion-weighted imaging analysis of diffusion and microperfusion in grading gliomas and comparison with arterial spin labeling for evaluation of tumor perfusion[J]. J MAGN RESON IMAGING 2016, **44**(3)**:** 620-632.
8. Bane O, Wagner M, Zhang JL, Dyvorne HA, Orton M, Rusinek H, Taouli B. Assessment of renal function using intravoxel incoherent motion diffusion-weighted imaging and dynamic contrast-enhanced MRI[J]. J MAGN RESON IMAGING 2016, **44**(2)**:** 317-326.
9. Shirota N, Saito K, Sugimoto K, Takara K, Moriyasu F, Tokuuye K. Intravoxel incoherent motion MRI as a biomarker of sorafenib treatment for advanced hepatocellular carcinoma: a pilot study[J]. CANCER IMAGING 2016, **16:** 1.
10. Barbieri S, Donati OF, Froehlich JM, Thoeny HC. Comparison of Intravoxel Incoherent Motion Parameters across MR Imagers and Field Strengths: Evaluation in Upper Abdominal Organs[J]. RADIOLOGY 2016, **279**(3)**:** 784-794.
11. Tao WJ, Zhang HX, Zhang LM, Gao F, Huang W, Liu Y, Zhu Y, Bai GJ. Combined application of pharamcokinetic DCE-MRI and IVIM-DWI could improve detection efficiency in early diagnosis of ductal carcinoma in situ[J]. J APPL CLIN MED PHYS 2019, **20**(7)**:** 142-150.
12. Wei Y, Huang Z, Tang H, Deng L, Yuan Y, Li J, Wu D, Wei X, Song B. IVIM improves preoperative assessment of microvascular invasion in HCC[J]. EUR RADIOL 2019, **29**(10)**:** 5403-5414.
13. Sun H, Xu Y, Song A, Shi K, Wang W. Intravoxel Incoherent Motion MRI of Rectal Cancer: Correlation of Diffusion and Perfusion Characteristics With Prognostic Tumor Markers[J]. AJR Am J Roentgenol 2018, **210**(4)**:** W139-W147.
14. Jungmann PM, Pfirrmann C, Federau C. Characterization of lower limb muscle activation patterns during walking and running with Intravoxel Incoherent Motion (IVIM) MR perfusion imaging[J]. MAGN RESON IMAGING 2019, **63:** 12-20.
15. Zhu G, Heit JJ, Martin BW, Marcellus DG, Federau C, Wintermark M. Optimized Combination of bvalues for IVIM Perfusion Imaging in Acute Ischemic Stroke Patients[J]. CLIN NEURORADIOL 2020,

30(3)**:** 535-544.

16. Sung JK, Jee WH, Jung JY, Choi M, Lee SY, Kim YH, Ha KY, Park CK. Differentiation of acute osteoporotic and malignant compression fractures of the spine: use of additive qualitative and quantitative axial diffusion-weighted MR imaging to conventional MR imaging at 3.0 T[J]. RADIOLOGY 2014, **271**(2)**:** 488-498.
17. Paschoal AM, Leoni RF, Dos SA, Paiva FF. Intravoxel incoherent motion MRI in neurological and cerebrovascular diseases[J]. Neuroimage Clin 2018, **20:** 705-714.
18. Ding Y, Tan Q, Mao W, Dai C, Hu X, Hou J, Zeng M, Zhou J. Differentiating between malignant and benign renal tumors: do IVIM and diffusion kurtosis imaging perform better than DWI? [J] EUR RADIOL 2019, **29**(12)**:** 6930-6939.
19. Klauss M, Maier-Hein K, Tjaden C, Hackert T, Grenacher L, Stieltjes B. IVIM DW-MRI of autoimmune pancreatitis: therapy monitoring and differentiation from pancreatic cancer[J]. EUR RADIOL 2016, **26**(7)**:** 2099-2106.
20. Zhu L, Wang H, Zhu L, Meng J, Xu Y, Liu B, Chen W, He J, Zhou Z, Yang X. Predictive and prognostic value of intravoxel incoherent motion (IVIM) MR imaging in patients with advanced cervical cancers undergoing concurrent chemo-radiotherapy[J]. Sci Rep 2017, **7**(1)**:** 11635.
21. Pui MH, Mitha A, Rae WI, Corr P. Diffusion-weighted magnetic resonance imaging of spinal infection and malignancy[J]. J NEUROIMAGING 2005, **15**(2)**:** 164-170.
22. Chan JH, Peh WC, Tsui EY, Chau LF, Cheung KK, Chan KB, Yuen MK, Wong ET, Wong KP. Acute vertebral body compression fractures: discrimination between benign and malignant causes using apparent diffusion coefficients[J]. Br J Radiol 2002, **75**(891)**:** 207-214.
23. Kang KM, Lee JM, Yoon JH, Kiefer B, Han JK, Choi BI. Intravoxel incoherent motion diffusion-weighted MR imaging for characterization of focal pancreatic lesions[J]. RADIOLOGY 2014, **270**(2)**:** 444-453.
24. Lu Y, Jansen JF, Mazaheri Y, Stambuk HE, Koutcher JA, Shukla-Dave A. Extension of the intravoxel incoherent motion model to non-gaussian diffusion in head and neck cancer[J]. J MAGN RESON IMAGING 2012, **36**(5)**:** 1088-1096.
25. Mao X, Zou X, Yu N, Jiang X, Du J. Quantitative evaluation of intravoxel incoherent motion diffusion-weighted imaging (IVIM) for differential diagnosis and grading prediction of benign and malignant breast lesions. Medicine[J]. (Baltimore) 2018, **97**(26)**:** e11109.

Tables

Table 1 Patient demographics

Patient group	No. of patients	Male	Female	Mean age (yrs)[a]
Tuberculous Spondylitis	20	11	9	48.82 ± 19.84
spinal metastasis	50	30	20	56.92 ± 9.29
lung cancer	32	20	12	57.66 ± 9.40
breast cancer	7	0	7	53.29 ± 9.55
renal cancer	11	10	1	57.09 ± 9.12

Note: [a] Data are means ± standard deviations

Table 2 IVIM parameters among tuberculous spondylitis and spinal metastasis

Patient group	ADC_{stand} ($\times10^{-3}$ mm^2/s)	ADC_{slow} ($\times10^{-3}$ mm^2/s)	ADC_{fast} ($\times10^{-3}$ mm^2/s)	f	DDC ($\times10^{-3}$ mm^2/s)	α
Tuberculous spondylitis	1.11 ± 0.25	0.77 ± 0.35	21.96 ± .782	0.45 ± 0.20	1.22 ± 0.34	0.77 ± 0.10
Spinal metastasis	1.05 ± 0.27	0.85 ± 0.28	33.87 ± 6.87	0.25 ± 0.15	1.17 ± 0.44	0.75 ± 0.09
lung cancer	0.95 ± 0.23	0.73± 0.23	33.31 ± 5.44	0.27 ± 0.18	0.99 ± 0.29	0.78 ± 0.07
breast cancer	1.20 ± 0.30	1.05 ± 0.29	36.96 ± 10.45	0.22 ± 0.14	1.60 ± 0.50	0.75 ± 0.08
renal cancer	1.25 ± 0.23	0.82 ± 0.30	30.46 ± 8.93	0.31 ± 0.19	1.19 ± 0.41	0.76 ± 0.09

Table 3 Comparison of mean IVIM-parameters for tuberculous spondylitis and spinal metastasis

Parameters	t	*p*
ADC_{stand}	0.855	0.395
ADC_{slow}	-1.017	0.313
ADC_{fast}	-6.296	<0.0001**
f	4.645	<0.0001**
DDC	0.399	0.691
α	0.854	0.396

Note: **p < 0.0001

Table 4. The result of Logistic regression model

Parameters	B	S.E.	Wald	*p*	OR	95% C.I.OR	
ADC_{fast}	-6.185	2.408	6.597	0.010*	0.002	0.001	0.231
f	0.235	0.068	11.847	0.001*	1.265	1.107	1.446

Note: *p < 0.05

Table 5. Efficacy of IVIM in the differential diagnosis of tuberculous spondylitis and spinal metastasis

Parameters	AUC (95%CI)	Cut-off values	Sensitivity (95%CI)	Specificity (95%CI)
ADC_{fast}	0.876 (0.782~0.969)	> 29.05	80.0 (66.3~90.0)	85.0 (62.1~96.6)
f	0.823 (0.719~0.927)	< 0.4	86.0 (73.3~94.2)	65.0 (40.8~84.5)
ADC_{fast} and f	0.925 (0.858~0.992)		94.0 (83.4~98.7)	80.0(56.3~94.1)

Figures

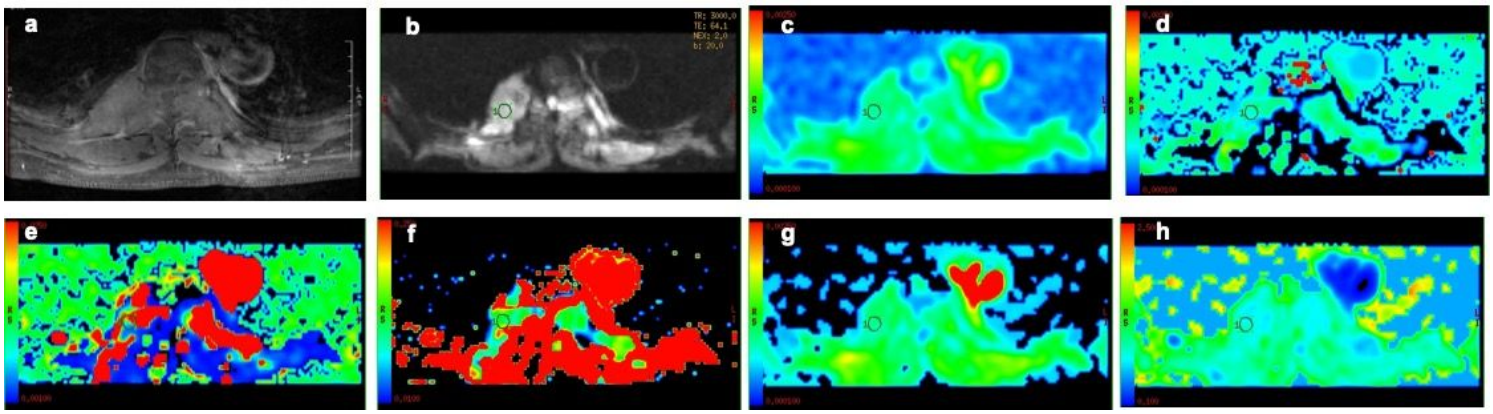

Figure 1

A 53-year-old man with spinal metastasis from lung cancer. The lesion showed obvious enhancement on T1WI (a) and hyperintensity on DWI (b). ADC values were 0.926×10−3 mm2/s (c). ROI was placed on DWI (b) and copied it to the other IVIM parametric maps of ADCslow, ADCfast, f, DDC and α (d–h) with values of 0.8×10−3 mm2/s, 0.0211 mm2/s, 0.139, 0.945×10−3 mm2/s and 0.759, respectively.

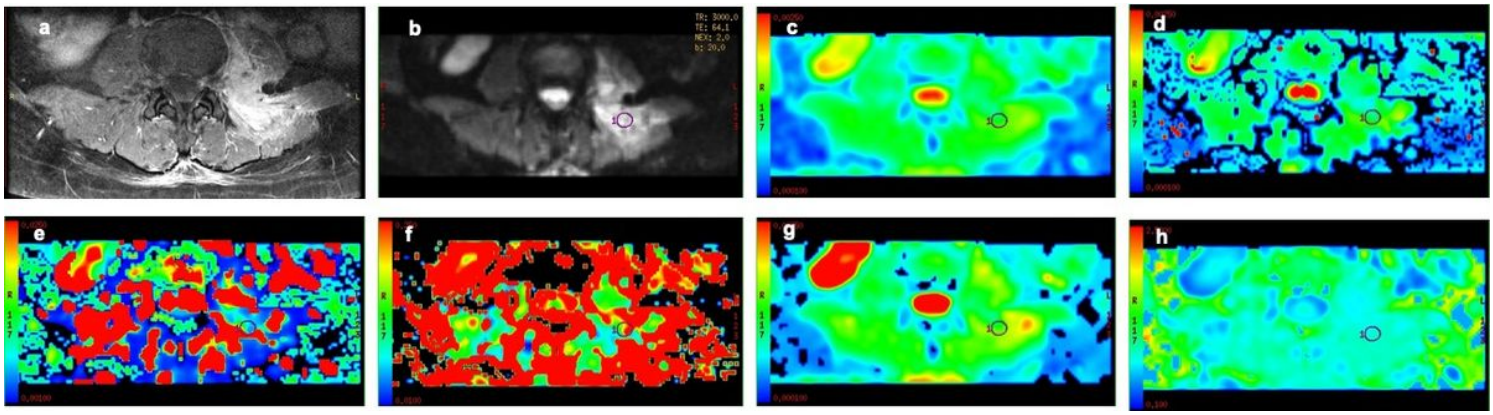

Figure 2

A 44-year-old woman with spinal tuberculosis. The lesion showed obvious enhancement on T1WI (a) and hyperintensity on DWI (b). ADC values were 1.28×10−3 mm2/s (c). ROI was placed on DWI (b) and copied it to the other IVIM parametric maps of ADCslow, ADCfast, f, DDC and α (d–h) with values of 1.11×10−3 mm2/s, 0.0131 mm2/s, 0.190, 1.41×10−3 mm2/s and 0.807, respectively.

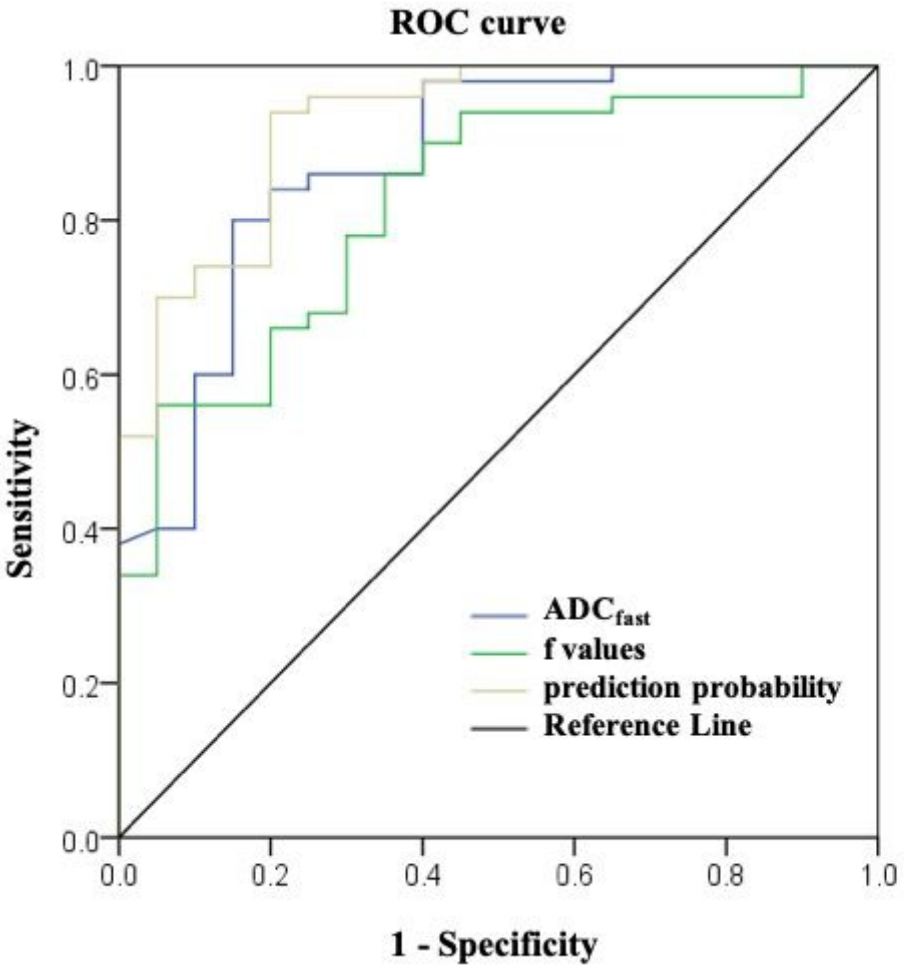

Figure 3

ROC curves for differentiating tuberculous spondylitis and spinal metastasis